

1 **Virological Characterization of a New Isolated Strain of Andes Virus Involved in**  
2 **the Recent Person-to-Person Transmission Outbreak Reported in Argentina**

3 Rocío M. Coelho<sup>1‡</sup>, Sebastian Kehl<sup>1‡</sup>, Natalia Periolo<sup>1</sup>, Emiliano Biondo<sup>2</sup>, Daniel O.  
4 Alonso<sup>1</sup>, Celeste Perez<sup>3</sup>, Darío Fernández Do Porto<sup>4,5</sup>, Gustavo Palacios<sup>6</sup>, Alexis  
5 Edelstein<sup>7</sup>, Carla Bellomo<sup>1</sup>, Valeria P. Martinez<sup>1,\*</sup>

6  
7 <sup>1</sup> Molecular Biology Service, Virology Department, Administración Nacional de  
8 Laboratorios e Institutos de Salud "Dr. C. G. Malbrán", Ciudad Autónoma de Buenos  
9 Aires C1282 AFF, Argentina;

10 <sup>2</sup> Área Programática de Esquel, Secretaria de Salud Chubut, Esquel, Chubut U 9200,  
11 Argentina;

12 <sup>3</sup> Tissue Culture Service, Virology Department, Administración Nacional de  
13 Laboratorios e Institutos de Salud "Dr. C. G. Malbrán", Ciudad Autónoma de Buenos  
14 Aires C1282 AFF, Argentina;

15 <sup>4</sup> Facultad de Ciencias Exactas y Naturales, Universidad de Buenos Aires, Buenos Aires  
16 C1428, Argentina;

17 <sup>5</sup> Consejo Nacional de Investigaciones Científicas y Técnicas, Ciudad Autónoma de  
18 Buenos Aires C 1414, Argentina;

19 <sup>6</sup> Icahn School of Medicine at Mount Sinai, NY 10029, EE. UU.;

20 <sup>7</sup> Unidad Operativa Centro de Contención Biológica, Administración Nacional de  
21 Laboratorios e Institutos de Salud "Dr. C. G. Malbrán", Ciudad Autónoma de Buenos  
22 Aires C1282 AFF, Argentina.

23 \* Correspondence: pmartinez@anlis.gob.ar; Tel: +54 11 3751 8054 (Buenos Aires,  
24 Argentina)

25 ‡ These authors contributed equally to this work.

26

27 **Keywords**

28 Hantavirus; Andes virus; Hantavirus pulmonary syndrome; Infection diseases; culture  
29 isolation; Animal model; Hamster; person-to-person transmission.

30

### 31 **Summary**

32 On November 2018, a person-to-person transmission outbreak of Andes virus (ANDV)  
33 began in the small town of Epuyen, Argentina. The strain involved demonstrated a high  
34 capacity for sustained transmission among the human population requiring the  
35 implementation of quarantine measures, rigorous contact tracing, isolation of close  
36 contacts, and active clinical monitoring to prevent further spread. In this study, we  
37 report the isolation of this strain, which we name the ARG-Epuyen after just three  
38 passages in cell culture. Complete sequencing revealed only a single amino acid change  
39 post-isolation, revealing that it is a non-adapted, wild-type ANDV strain, and its  
40 isolation probably represents a critical step toward the development of medical  
41 countermeasures against this emerging pathogen. The pathogenicity and transmissibility  
42 potential of ARG-Epuyen were evaluated in hamsters, the only animal model for  
43 Hantavirus Pulmonary Syndrome. Additionally, this strain was compared with ARG, an  
44 ANDV strain previously isolated from the same geographical area in the Argentinian  
45 Patagonia, from a rodent specimen. Our findings revealed high infectiousness and  
46 efficient hamster-to-hamster transmission through direct contact experiments, although  
47 ARG-Epuyen appeared to be less pathogenic than ARG.

### 48 **1. Introduction**

49 Hantaviruses (*Bunyvirales: Hantaviridae: Mammantavirinae*) are enveloped, single  
50 stranded, negative sense RNA viruses with three-segmented genome. The genomic  
51 segments consist of a small segment (S), a medium segment (M), and a large segment  
52 (L), which encode the nucleocapsid (N) protein, a nonstructural protein (NSs) in some

53 species, surface glycoproteins (Gn and Gc), and an RNA-dependent RNA polymerase  
54 (RdRp), respectively (1). Hantaviruses are distributed worldwide and are hosted by  
55 various vertebrate animal species. Pathogenic hantaviruses are primarily associated with  
56 rodents as natural reservoirs and are classified under the genus *Orthohantavirus*. These  
57 viruses establish seemingly asymptomatic and chronic infections in several rodent  
58 species. The risks of viral spillover have increased due to new farming practices,  
59 climate change, the expansion of rural human settlements, and disruptions to the  
60 zoonotic interface. Additionally, rural tourism has led to travel-related cases (2–4).  
61 Several species of orthohantaviruses are responsible for Hantavirus Pulmonary  
62 Syndrome (HPS) in the Americas and Hemorrhagic Fever with Renal Syndrome  
63 (HFRS) in Asia and Europe. HPS, first described in 1993 in the US (5), is caused by at  
64 least 24 distinct viruses (6). Humans generally become infected through the inhalation  
65 of aerosolized rodent excreta. In Argentina, most HPS cases are caused by seven viruses  
66 closely related to Andes virus (ANDV), species *Orthohantavirus andesense*. ANDV  
67 was the first hantavirus characterised in Argentina (7) and it was associated with the  
68 long-tailed pygmy rice rat *Oligoryzomys longicaudatus* in the Patagonian Andean  
69 region. The signs and symptoms of the disease can manifest after a long period of up to  
70 40 days after infection (8,9). ANDV-HPS is associated with high case-lethality rates  
71 ranging from 21–50% (10,11).  
72 Before 1996, the route of orthohantavirus transmission was considered strictly zoonotic,  
73 resulting in “Dead-End” human infections (7). However, in 1996, an ANDV-caused  
74 HPS outbreak began in the small city of El Bolsón and then expanded to distant cities,  
75 such as Bariloche (121 km) and Buenos Aires (1700 km), involving 16  
76 epidemiologically linked cases. This outbreak became a focal point for orthohantavirus  
77 research because molecular and epidemiological evidence suggested person-to-person

78 (PTP) transmission (12,13). A larger PTP transmission outbreak that began in 2018 and  
79 involved 34 cases, could be curtailed by the implementation of strict quarantine  
80 measures. In this outbreak, several individuals were identified as superspreaders,  
81 predicting the high transmission potential of this strain (10).  
82 To date, no vaccines or therapeutic treatments are available for any HPS agent,  
83 therefore, there is an urgent need for vaccine candidates and/or therapeutics. The  
84 paucity of vaccine developments relayed for many years on the lack of animal models,  
85 due to their zoonotic origin, and on the difficulty to isolate New World Hantaviruses in  
86 cell culture. Only three strains of ANDV had been propagated in cell culture (CH-  
87 9717869; CH-7913 and ARG). CHI-7913 was obtained from a serum sample of a  
88 Chilean patient before the onset of symptoms (14). CH-9717869 and ARG were isolated  
89 from long tailed pygmy rice rats captured in Chile and Argentina respectively (15,16). It  
90 was first described that CH-9717869, and later ARG, caused a lethal and very similar  
91 disease to HPS in Syrian Golden Hamsters (17,18) and, since then, the model  
92 ANDV/hamster became a unique resource for the study of HPS. Most recently, the  
93 human CHI-7913 strain resulted in an asymptomatic infection in the same animal model  
94 suggesting that the lethal ANDV model of HPS is strain specific, reinforcing the  
95 necessity to obtain and characterise new human strains of ANDV to understand their  
96 pathogenesis in humans (19). In this work we report the isolation in cell culture of the  
97 strain responsible for the largest ANDV PTP-transmission outbreak ever reported,  
98 ARG-Epuyen. In addition, we performed a preliminary virological characterization of  
99 this strain proving its ability to infect hamsters causing high levels of viremia and to  
100 spread efficiently between them through direct contact experiments.

## 101 **2. Materials and methods**

102 **2.1. Virus isolation on cell culture.** Biological samples involved in this study were  
103 obtained during the Ministry of Health activities for the epidemiological investigation of  
104 the PTP outbreak from November 2018 to March 2019. The specimens were originally  
105 obtained from living individuals in a form that neither the recipient nor the provider can  
106 link the biospecimens directly to identifiable private information of the original source.  
107 Unidentified remnant biological specimens were utilized for virus isolation. The  
108 samples with higher viral load and absence of antibodies were selected. Complete  
109 genome sequencing revealed 100% nucleotide identity with cases involved in the PTP  
110 transmission outbreak (8). The selected serum samples were inoculated onto Vero E6  
111 cell monolayer (CRL-1586; ATCC, Manassas, VA, USA) and incubated for one hour at  
112 37 °C in a humidified atmosphere containing 5% CO<sub>2</sub>. After the incubation, fresh  
113 complete medium (MEM, 10% FBS, antibiotics, and antimycotics) was added to each  
114 flask, and incubated at 37 °C under the same conditions. After 15 days, the cells were  
115 trypsinized, washed, and seeded onto a new monolayer, and incubated under identical  
116 conditions (first blind passage). For each flask, one-third of the cells were stored at -80  
117 °C, another third was tested by indirect immunofluorescence assay (IFA), and the final  
118 third was seeded onto a new monolayer. The medium was centrifuged, aliquoted, and  
119 stored at -80 °C. Three blind passages were performed in total. Each passage was  
120 monitored by real-time RT-PCR for ANDV RNA in the culture media and by IFA for  
121 detecting viral antigen in the cells. Mock-infected Vero E6 cells, treated under identical  
122 conditions, were used as a negative control.

123 **2.2. Immunofluorescence Assay.** Infected and mock-infected cells were resuspended  
124 in 1X phosphate-buffered saline (PBS) and washed three times by centrifugation at 400  
125 x g for five minutes at 4 °C. The pellets were then resuspended in 1 ml PBS, and several  
126 10 µl drops of each suspension were spotted onto a slide. The slides were left inside a

127 laminar flow cabinet until completely dried. The slides were then immersed in ice-cold  
128 acetone for 10 minutes at -20 °C, removed from the acetone, allowed to dry, and stored  
129 at -20 °C until further processing. The slides were blocked with 3% horse serum in  
130 PBS-Triton for 15 minutes at room temperature and then washed with PBS. The cells  
131 were treated with a 1:500 dilution of rabbit polyclonal serum against ANDV in PBS-  
132 Triton-BSA and incubated for one hour at 37 °C in a humid chamber. After washing,  
133 the slides were incubated with FITC-conjugated anti-rabbit IgG (Kirkegaard & Perry) in  
134 PBS-Triton-BSA under the same conditions. Finally, the cells were incubated with 1  
135 µg/ml DAPI in PBS for 15 minutes at room temperature and then washed. The slides  
136 were allowed to drain, mounted, and analyzed under a fluorescent microscope.

137 **2.3. Virus infection in Vero E6 and A549 cell lines.** Vero E6 and A549 (human  
138 epithelial lung cell, ATCC CCL-185) cells were maintained in Dulbecco's Modified  
139 Eagle's Medium (DMEM high glucose; Sigma) supplemented with 5% fetal bovine  
140 serum (FBS, Gibco), 10 mM HEPES buffer, and 2 mM L-glutamine. The cells were  
141 infected with ARG and ARG-Epuyen at the indicated multiplicity of infection (MOI)  
142 for 60 minutes at 37 °C. After incubation, the monolayers were washed three times with  
143 PBS, and the cells were maintained in complete DMEM (Sigma). Supernatants were  
144 collected at various days post-infection, centrifuged to remove cells, and stored at -80  
145 °C until use. Viral RNA was isolated using the Qiagen QIAamp® Viral RNA kit  
146 according to the manufacturer's protocol. Viral growth kinetics were determined by  
147 quantifying ANDV RNA at different days post-infection using real-time RT-PCR as  
148 described below.

149 **2.4. Evaluation of ARG-Epuyen virulence in the hamster model.** To evaluate  
150 whether ANDV could be transmitted between hamsters in a manner similar to human  
151 transmission, Syrian Golden Hamsters were infected with either the ARG-Epuyen or

152 ARG strains. Seventeen 9-week-old hamsters were distributed across seven ventilated  
153 cages. One hamster per cage was infected via intramuscular injection (rear thigh) with  
154 100  $\mu$ l ( $1 \times 10^4$  FFU) of ARG-Epuyen passage No. 4 (two males and four females) or  
155 ARG passage No. 19 (one male). The infected hamsters were placed in direct contact  
156 with one or two non-infected individuals in the same ventilated cages on the day they  
157 were inoculated (day 0). As a control group, four hamsters were inoculated with cell  
158 culture supernatant from non-infected Vero E6 cells. All individuals were monitored  
159 daily for 30 days for signs of disease, including fatigue, inappetence, lethargy  
160 (reluctance to move), and/or dyspnea. Animals with fatal outcomes were necropsied on  
161 the day of death to collect lung samples, which were stored at -80 °C until processing.  
162 On day 30, all survivors were anesthetized by inhalation of isoflurane, terminally bled  
163 by cardiac puncture, and necropsied to obtain lung tissue.

164 **2.5. Enzyme Linked Immunosorbent Assay.** The detection of IgG antibodies against  
165 the viral nucleoprotein (NP) in hamsters was performed by ELISA, as previously  
166 described, to confirm infection (18). Briefly, serial dilutions of hamster sera were  
167 incubated in polystyrene plates coated with recombinant ANDV-NP and a nonspecific  
168 recombinant protein in a humid chamber at 37 °C for 1 hour. After washing,  
169 peroxidase-labelled goat anti-hamster IgG (H+L) (Kirkegaard & Perry) was added and  
170 incubated under the same conditions. TMB solution was used as a substrate, and optical  
171 density (OD) was measured at 450 nm.  $\Delta$ OD values were calculated by subtracting the  
172 OD measured for each sample incubated with the specific (ANDV-NP) and nonspecific  
173 recombinant proteins. Samples were considered IgG positive if  $\Delta$ OD values were  
174 greater than 0.4. The IgG titre was calculated as the inverse of the highest dilution that  
175 yielded a positive result.

176 **2.6. Viral RNA detection and genomic sequencing.** Total RNA was extracted from  
177 lung samples and from the culture medium of infected cell passages using Trizol  
178 (Invitrogen) according to the manufacturer's protocol. RT-qPCR was performed as  
179 previously described (20). Briefly, each RNA sample was amplified in duplicate using  
180 the One Step RT-qPCR qScript kit (Quanta Biosciences) following the manufacturer's  
181 instructions. Each reaction mixture contained 12.5 µl of 2X Master Mix, 2 µl of an  
182 oligonucleotide mix designed to amplify the ANDV S-segment (1 µM each), 4.75 µl of  
183 nuclease-free water, 0.5 µl of the ANDV probe (5' FAM-BHQ-3'), 0.25 µl of qScript  
184 One Step RT, and 5 µl of template RNA. Reverse transcription was performed at 50 °C  
185 for 15 minutes, followed by denaturation at 95 °C for 5 minutes, and 40 cycles of  
186 amplification at 95 °C for 15 seconds and 60 °C for 60 seconds in a Real-Time PCR  
187 Detection System CFX-96 (Bio-Rad, CA). To obtain complete genomic sequences, an  
188 amplicon-based method was selected using a one-step RT-PCR strategy to enrich  
189 vRNA, followed by library preparation as previously described (21). The library was  
190 sequenced on a MiSeq sequencing platform (Illumina, San Diego, CA) using 2 x 151-bp  
191 paired-end sequencing. Bioinformatic analysis was performed as described previously  
192 (8).

193 **2.7. Biosafety precautions and Ethics statements.** The entire procedure of viral  
194 isolation, subsequent propagation, and sample analysis before viral inactivation was  
195 conducted at the biosafety level 3 facility at the Unidad Operativa Centro de Contención  
196 Biológica (UOCCB-ANLIS). All procedures involving human samples for viral  
197 isolation used in this study were approved by the Bioethics Committee, Area  
198 Programatica Comodoro Rivadavia, Chubut province, to ensure compliance with ethical  
199 standards. All procedures involving animal handling were carried out within an animal



200 biosafety level 3 facility at UOCCB-ANLIS and hamsters were housed in ventilated  
201 cage racks. Research was conducted in compliance with institutional guidelines  
202 and the national law no.: 14,346, that regulates experiments involving animals, and  
203 adheres to principles stated in the Guide for the Care and Use of Laboratory Animals,  
204 National Research Council, 2011 (22). An institutional committee for animal use and  
205 care approved the protocols used.

### 206 **3. Results**

#### 207 **3.1. A new strain of Andes virus was isolated in cell culture from a human serum**

208 **sample.** A human serum sample with a high viral load ( $6.3 \times 10^7$  copies/ml) and no  
209 detectable specific antibodies against ANDV, was selected to infect a Vero E6 cell  
210 monolayer. After three blind passages, viral RNA was detectable in the supernatant of  
211 the infected cell culture ( $2.5 \times 10^8$  copies/ml). Infection was confirmed in the cells by  
212 IFA, showing the presence of viral antigen in approximately 50% of the cells in passage  
213 No. 3 and 80% in passage No. 4 (p4) (Figure 1). A large viral stock was prepared from  
214 the supernatant of passage No. 3, as described above, for use in subsequent experiments.  
215 The infectious titre of the viral stock obtained was  $2.1 \times 10^6$  FFU/ml. This new strain  
216 was designated as ARG-Epuyen.

#### 217 **3.2. ARG-Epuyen and ARG showed differential kinetics of replication and**

218 **infectivity in cell cultures.** The growth kinetics of the ARG and ARG-Epuyen strains  
219 were first assessed in Vero E6 cells using an MOI of 0.002 (Figure 2). Quantification of  
220 viral RNA in the culture supernatants of cells infected with each strain showed that  
221 ARG replicates faster than ARG-Epuyen. Both strains produced high levels of  
222 infectious viral particles, with the maximum level observed for ARG, which reached up  
223 to  $2.1 \times 10^7$  FFU/ml, whereas ARG-Epuyen did not exceed  $2.1 \times 10^6$  FFU/ml (Figure  
224 2B). The growth kinetics were then compared using the epithelial cell line A549 with a

225 higher MOI. The results were consistent, showing that ARG replicates faster than ARG-  
226 Epuyen in both Vero E6 and A549 cells (Figure 3).

227 **3.3. Both strains of Andes virus are highly transmissible in Hamsters.** Seven Syrian

228 Golden hamsters of different sexes (3 males: MI; 4 females: FI) were inoculated  
229 intramuscularly with high doses of ANDV (approximately  $1 \times 10^4$  FFU) and placed in  
230 separate cages with one or two non-inoculated cage-mates (receptors: MR and FR).

231 During the 30 days post-infection (p.i.) period, neither the hamsters inoculated with  
232 ARG-Epuyen (n=6) nor the receptors exposed to them (n=9) showed any visible signs  
233 of illness. However, infection was confirmed in all of them through seroconversion  
234 and/or genomic RNA detection in lung tissues (Table 1). In contrast, the single hamster  
235 inoculated with ARG (MI-1) exhibited inappetence and lethargy starting from day five  
236 p.i., and dyspnea was evident from day 13 to day 16 p.i. After 11 days of illness, MI-1  
237 gradually improved and fully recovered by the end of the experiment. However, the two  
238 hamsters exposed to MI-1, MR-1 and MR-2, became ill 16 and 22 days after the onset  
239 of symptoms in MI-1, respectively, and both rapidly died. After 30 days p.i., all the  
240 survivors were sampled and sacrificed. The six index hamsters showed a strong humoral  
241 response (IgG titers  $>25,600$ ), while four out of 11 of their cage-mates (receptors)  
242 exhibited low to moderate IgG titers. Nevertheless, all of them (n=11) were infected, as  
243 evidenced by the detection of viral RNA in blood (up to  $1.5 \times 10^7$  RNA copies/ml)  
244 and/or in lung tissues (up to  $1.6 \times 10^8$  copies/100 ng RNA).

245 **3.4. ARG-Epuyen grew in cell culture without need of adaptation.** To analyze  
246 potential changes that could lead to viral adaptation for growth in cell culture and  
247 replication in hamsters, the complete genomes of the isolated virus (p4) and from the  
248 lung of an infected hamster (MI-3) were sequenced and compared with the previously  
249 published sequence from the human sample (GenBank MN258238, MN258204,

250 MN258171). The isolated strain ARG-Epuyen p4 showed only one nucleotide change in  
251 the non-coding region of the S segment (position 1522) and one non-synonymous  
252 change, K2116E, in the L segment (A6381G). No changes were observed between the  
253 isolated strain (p4) and the virus recovered from the infected hamster.

254 To investigate the molecular basis for the observed differences in pathogenicity between  
255 ARG-Epuyen (p4) and ARG (p19) in the hamster model, we compared the complete  
256 sequences of both strains. We identified 25 non-synonymous substitutions: three in the  
257 S segment (one in the N ORF and two in the NSs ORF), 10 in the M segment (six in Gn  
258 and four in Gc), and 12 in the L segment (Table 2).

#### 259 **4. Discussion.**

260 The limited progress in vaccine development and other medical countermeasures  
261 (MCMs) against hantaviruses has been partly due to restricted access to wild-type viral  
262 strains and the lack of appropriate animal models of the disease. Additionally, no  
263 reverse genetic system for hantaviruses has been reported to date. Generally, in vivo and  
264 in vitro studies of hantavirus infections have been conducted using cell-cultured strains  
265 derived from moderate to high passage numbers. The success of MCM development  
266 depends on selecting strains that are actively circulating and have proven pathogenicity  
267 in humans.

268 Following the COVID-19 pandemic, the National Institute of Allergy and Infectious  
269 Diseases proposed a prototype pathogen approach to develop a generalizable MCM  
270 strategy. This approach can be applied to other viruses within the same viral family,  
271 enabling the rapid development of MCMs and shortening the timeline between  
272 pathogen outbreak and regulatory authorization if a virus with similar properties  
273 emerges. ANDV has been mentioned as a prototype pathogen of the Hantaviridae  
274 family and should be considered for vaccine development and pre-clinical and clinical

275 testing (23,24). For these purposes, the availability of well-characterized ANDV strains  
276 is critical.

277 In this work, we described the isolation of the strain responsible for the largest ANDV  
278 PTP transmission outbreak, which occurred in the small town of Epuyen and began on 2  
279 November 2018. This strain, ARG-Epuyen, exhibited a high capacity for PTP  
280 transmission, necessitating the implementation of quarantine measures to curtail further  
281 spread (8). The median reproductive number (the mean number of secondary cases  
282 caused by an infected person) was 2.12 before control measures were implemented and  
283 subsequently dropped to below 1.0 by late January. Early intervention allowed for the  
284 collection of samples leading to the isolation of this new ANDV strain from an  
285 asymptomatic case. An early passage of this strain was sequenced, revealing only one  
286 amino acid difference from the virus recovered from the patient, indicating that it can be  
287 considered a wild-type strain. Like the ARG strain, this strain was able to grow in a new  
288 host without needing adaptation (25).

289 Two of the three previously isolated ANDV strains in cell culture caused lethal disease  
290 in hamsters (17–19,25). Although this animal model has become crucial for studying  
291 the pathogenesis of HPS, the spreading capacity and horizontal transmission of ANDV  
292 have only been evaluated in one previous study with the CH-9717869 strain (26). In this  
293 study, we assessed the pathogenicity and spreading capacity of the strain responsible for  
294 sustained PTP transmission in this animal model and compared it with the highly lethal  
295 ARG strain in direct exposure experiments. All hamsters—both those directly  
296 inoculated and those exposed to infected hamsters—became infected. Our data  
297 indicated that ARG-Epuyen was less virulent than ARG, as none of the six index  
298 hamsters inoculated with ARG-Epuyen developed severe disease during the 30-day  
299 period, despite showing high viral titres in blood and lungs. However, as five hamsters

300 exposed to the index hamsters were sacrificed during the incubation period—when they  
301 had no IgG titres and rising viral RNA loads in blood and lungs—their final outcomes  
302 could not be assessed. We demonstrated that both ARG and ARG-Epuyen were highly  
303 transmissible in direct exposure experiments. Although the mechanism of transmission  
304 remains to be confirmed through indirect exposure experiments, we hypothesize that the  
305 route was likely respiratory or digestive, due to the absence of wounds in the animals.  
306 Further studies are required to assess the pathogenic characteristics of this strain in the  
307 animal model.

308 Our preliminary data revealed differences in lethality between the two Argentinean  
309 strains. A previous comparative study of two Chilean strains found similar results. The  
310 strain obtained from a human serum sample (CHI-7913) caused an asymptomatic  
311 infection in hamsters, while the strain obtained from a rodent (CHI-9717869) was  
312 highly lethal (19). The molecular basis for the observed differences in pathogenesis  
313 between these strains was evaluated through in silico studies (19,25). However, the  
314 specific differences observed need further investigation through directed mutagenesis  
315 experiments. The N protein plays no role, as both strains share 100% identity. In vitro  
316 studies suggested that ANDV virulence could be determined by its ability to alter  
317 cellular signalling pathways by restricting the early induction of beta interferon (IFNB)  
318 and IFN-stimulated genes (ISGs) (26–28). Additionally, compared with other  
319 pathogenic hantaviruses, ANDV is unique in that three viral proteins—N, NSs, and  
320 Gn/Gc—can block the same signalling pathway at different levels. However, the few  
321 differences found in the Gn/Gc between the strains seem to be located outside  
322 conserved motifs or domains involved in the regulation of the IFNB response. Further  
323 characterization of the NSs and RdRp proteins is needed to evaluate the effects of the  
324 observed changes.

325 As a result of comparing the complete sequences of both ANDV strains, several amino  
326 acid changes were predicted. None of the substitutions represented drastic changes that  
327 could affect key motifs already described for the structural conformation and/or  
328 function of the N, Gn/Gc, and RdRp proteins. Exceptions included the changes P97S  
329 and T641I in the M-segment; the P residue is in the Gn ectodomain and may impact the  
330 flexibility of a loop structure, affecting recognition by some immune response  
331 components and/or interaction with cell receptors. The T641I change, located in an  
332 alpha-helix structure near the WAASA motif, may result in the loss of an oxygen  
333 molecule capable of forming a hydrogen bond with the adjacent residue C642.  
334 In conclusion, we obtained a low-passaged isolate of a prototype pathogen: ANDV. The  
335 new strain, ARG-Epuyen, is a well-characterized isolate due to its known outcome in a  
336 recent HPS outbreak and its high PTP transmission potential. Furthermore, the isolation  
337 was obtained directly from a clinical sample with a low number of passages (p=4) and  
338 only one amino acid change. Therefore, it can be considered an ANDV wild-type strain,  
339 representing a critical step toward developing MCMs against this emerging pathogen.

340

#### 341 **Acknowledgments**

342 We thank Silvia Girard and Lara Martín for laboratory support.

343 Financial support: this work was supported by the Instituto Nacional de Enfermedades  
344 Infecciosas, Administración Nacional de Laboratorios e Institutos de Salud "Dr. C.  
345 Malbrán".

346 All authors: No reported conflicts of interest.

#### 347 **Biographical Sketch**

348 Miss Coelho and Mr. Kehl are part of the staff of the Hantavirus National Reference  
349 Laboratory. Coelho's primary research interests include diagnoses of infectious diseases

350 and is coordinating the serology section of the laboratory. Mr. Kehl is a junior  
351 researcher interested in infectious diseases and emergent viral zoonosis.

352

## 353 REFERENCES

- 354 1. Plyusnin A, Vapalahti O, Vaheri A. Hantaviruses: genome structure, expression and  
355 evolution. *J Gen Virol.* noviembre de 1996;77 ( Pt 11):2677-87.
- 356 2. Castillo C, Nicklas C, Mardones J, Ossa G. Andes Hantavirus as possible cause of  
357 disease in travellers to South America. *Travel Med Infect Dis.* enero de  
358 2007;5(1):30-4.
- 359 3. Kuenzli AB, Marschall J, Schefold JC, Schafer M, Engler OB, Ackermann-  
360 Gäumann R, et al. Hantavirus Cardiopulmonary Syndrome Due to Imported Andes  
361 Hantavirus Infection in Switzerland: A Multidisciplinary Challenge, Two Cases and  
362 a Literature Review. *Clin Infect Dis Off Publ Infect Dis Soc Am.* 13 de noviembre  
363 de 2018;67(11):1788-95.
- 364 4. Kofman A, Eggers P, Kjemtrup A, Hall R, Brown SM, Morales-Betoulle M, et al.  
365 Notes from the Field: Contact Tracing Investigation after First Case of Andes Virus  
366 in the United States - Delaware, February 2018. *MMWR Morb Mortal Wkly Rep.*  
367 19 de octubre de 2018;67(41):1162-3.
- 368 5. Nichol ST, Spiropoulou CF, Morzunov S, Rollin PE, Ksiazek TG, Feldmann H,  
369 et al. Genetic identification of a hantavirus associated with an outbreak of acute  
370 respiratory illness. *Science.* 5 de noviembre de 1993;262(5135):914-7.
- 371 6. Abudurexiti A, Adkins S, Alioto D, Alkhovsky SV, Avšič-Županc T, Ballinger MJ,  
372 et al. Taxonomy of the order Bunyavirales: update 2019. *Arch Virol.* julio de  
373 2019;164(7):1949-65.
- 374 7. López N, Padula P, Rossi C, Lázaro ME, Franze-Fernández MT. Genetic  
375 identification of a new hantavirus causing severe pulmonary syndrome in  
376 Argentina. *Virology.* 1 de junio de 1996;220(1):223-6.
- 377 8. Martínez VP, Di Paola N, Alonso DO, Pérez-Sautu U, Bellomo CM, Iglesias AA,  
378 et al. «Super-Spreaders» and Person-to-Person Transmission of Andes Virus in  
379 Argentina. *N Engl J Med.* 3 de diciembre de 2020;383(23):2230-41.
- 380 9. Iglesias AA, Períolo N, Bellomo CM, Lewis LC, Olivera CP, Anselmo CR, et al.  
381 Delayed viral clearance despite high number of activated T cells during the acute

- 382 phase in Argentinean patients with hantavirus pulmonary syndrome. *EBioMedicine*.  
383 2 de enero de 2022;75:103765.
- 384 10. Martinez VP, Bellomo CM, Cacace ML, Suarez P, Bogni L, Padula PJ. Hantavirus  
385 pulmonary syndrome in Argentina, 1995-2008. *Emerg Infect Dis*. diciembre de  
386 2010;16(12):1853-60.
- 387 11. Tortosa F, Carrasco G, Gallardo D, Prandi D, Parodi V, Santamaría G, et al.  
388 [Prognostic factors for cardio-pulmonary syndrome and death by hantavirus Andes  
389 Sur: cohort study in San Carlos de Bariloche and health influence area]. *Medicina*  
390 (Mex). 2022;82(3):351-60.
- 391 12. Wells RM, Sosa Estani S, Yadon ZE, Enria D, Padula P, Pini N, et al. An unusual  
392 hantavirus outbreak in southern Argentina: person-to-person transmission?  
393 Hantavirus Pulmonary Syndrome Study Group for Patagonia. *Emerg Infect Dis*.  
394 junio de 1997;3(2):171-4.
- 395 13. Padula PJ, Edelstein A, Miguel SD, López NM, Rossi CM, Rabinovich RD.  
396 Hantavirus pulmonary syndrome outbreak in Argentina: molecular evidence for  
397 person-to-person transmission of Andes virus. *Virology*. 15 de febrero de  
398 1998;241(2):323-30.
- 399 14. Galeno H, Mora J, Villagra E, Fernandez J, Hernandez J, Mertz GJ, et al. First  
400 human isolate of Hantavirus (Andes virus) in the Americas. *Emerg Infect Dis*. julio  
401 de 2002;8(7):657-61.
- 402 15. Padula PJ, Sanchez AJ, Edelstein A, Nichol ST. Complete nucleotide sequence of  
403 the M RNA segment of Andes virus and analysis of the variability of the termini of  
404 the virus S, M and L RNA segments. *J Gen Virol*. septiembre de 2002;83(Pt  
405 9):2117-22.
- 406 16. Meissner JD, Rowe JE, Borucki MK, St Jeor SC. Complete nucleotide sequence of  
407 a Chilean hantavirus. *Virus Res*. octubre de 2002;89(1):131-43.
- 408 17. Hooper JW, Larsen T, Custer DM, Schmaljohn CS. A lethal disease model for  
409 hantavirus pulmonary syndrome. *Virology*. 10 de octubre de 2001;289(1):6-14.
- 410 18. Martinez VP, Padula PJ. Induction of protective immunity in a Syrian hamster  
411 model against a cytopathogenic strain of Andes virus. *J Med Virol*. enero de  
412 2012;84(1):87-95.
- 413 19. Warner BM, Sloan A, Deschambault Y, Dowhanik S, Tierney K, Audet J, et al.  
414 Differential pathogenesis between Andes virus strains CHI-7913 and Chile-  
415 9717869in Syrian Hamsters. *J Virol*. 24 de febrero de 2021;JVI.00108-21.



- 416 20. Bellomo CM, Pires-Marczeski FC, Padula PJ. Viral load of patients with hantavirus  
417 pulmonary syndrome in Argentina. *J Med Virol.* noviembre de 2015;87(11):1823-  
418 30.
- 419 21. Alonso DO, Kehl S, Coelho R, Periolo N, Poklepovich T, Perez-Sautu U, et al.  
420 Orthohantavirus Diversity in Central-East Argentina: Insights from Complete  
421 Genomic Sequencing on Phylogenetics, Geographic patterns and Transmission  
422 scenarios. *bioRxiv.* 1 de enero de 2024;2024.03.25.586579.
- 423 22. National Research Council (US) Committee for the Update of the Guide for the Care  
424 and Use of Laboratory Animals. *Guide for the Care and Use of Laboratory Animals*  
425 [Internet]. 8th ed. Washington (DC): National Academies Press (US); 2011 [citado  
426 20 de agosto de 2024]. (The National Academies Collection: Reports funded by  
427 National Institutes of Health). Disponible en:  
428 <http://www.ncbi.nlm.nih.gov/books/NBK54050/>
- 429 23. Cassetti MC, Pierson TC, Patterson LJ, Bok K, DeRocco AJ, Deschamps AM, et al.  
430 Prototype Pathogen Approach for Vaccine and Monoclonal Antibody Development:  
431 A Critical Component of the NIAID Plan for Pandemic Preparedness. *J Infect Dis.*  
432 15 de junio de 2023;227(12):1433-41.
- 433 24. Morabito KM, Cassetti MC, DeRocco AJ, Deschamps AM, Pierson TC. Viral  
434 Prototypes for Pandemic Preparedness: The Road Ahead. *J Infect Dis.* 18 de octubre  
435 de 2023;228(Suppl 6):S460-4.
- 436 25. Bellomo CM, Alonso DO, Pérez-Sautu U, Prieto K, Kehl S, Coelho RM, et al.  
437 Andes Virus Genome Mutations That Are Likely Associated with Animal Model  
438 Attenuation and Human Person-to-Person Transmission. *mSphere.* 22 de junio de  
439 2023;8(3):e0001823.
- 440 26. Riesle-Sbarbaro SA, Kirchoff N, Hansen-Kant K, Stern A, Kurth A, Prescott JB.  
441 Human-to-Human Transmission of Andes Virus Modeled in Syrian Hamsters.  
442 *Emerg Infect Dis.* octubre de 2023;29(10):2159-63.
- 443 27. Matthys VS, Cimica V, Dalrymple NA, Glennon NB, Bianco C, Mackow ER.  
444 Hantavirus GnT elements mediate TRAF3 binding and inhibit RIG-I/TBK1-directed  
445 beta interferon transcription by blocking IRF3 phosphorylation. *J Virol.* febrero de  
446 2014;88(4):2246-59.
- 447 28. Cimica V, Dalrymple NA, Roth E, Nasonov A, Mackow ER. An innate immunity-  
448 regulating virulence determinant is uniquely encoded by the Andes virus  
449 nucleocapsid protein. *mBio.* 18 de febrero de 2014;5(1):e01088-13.

- 450 29. Geimonen E, LaMonica R, Springer K, Farooqui Y, Gavrilovskaya IN, Mackow  
451 ER. Hantavirus pulmonary syndrome-associated hantaviruses contain conserved and  
452 functional ITAM signaling elements. *J Virol.* enero de 2003;77(2):1638-43.  
453

454 **TABLES**

**Table 1.** Evaluation of virulence of Andes virus strains in the golden hamster model.

Cage N°	Infected	Receptor	Sex	ANDV strain	IgG titer	viral RNA in blood (copies/ml)	vRNA in lung (copies/100 ng RNA)
1	MI-1		M	Andes/ARG	>25,600	$7.4 \times 10^6$	$1.35 \times 10^8$
		MR-1*	M		<100	NA	$8.5 \times 10^7$
		MR-2*	M		<100	NA	$5.2 \times 10^6$
2	FI-2		F	ARG-Epuyen	>25,600	$1.5 \times 10^7$	$5.3 \times 10^3$
		FR-3	F		400	ND	$7.2 \times 10^6$
3	MI-3		M	ARG-Epuyen	>25,600	$1.5 \times 10^7$	$1.5 \times 10^7$
		FR-4	F		6400	$7 \times 10^6$	$1.6 \times 10^8$
		FR-5	F		<100	$7.4 \times 10^6$	$4.3 \times 10^7$
4	FI-4		F	ARG-Epuyen	>25,600	$4.1 \times 10^6$	$1 \times 10^5$
		FR-6	F		<100	ND	$5.8 \times 10^3$
		FR-7	F		1600	$1 \times 10^7$	$7.8 \times 10^7$
5	FI-5		F	ARG-Epuyen	>25,600	$3.3 \times 10^6$	$3.4 \times 10^7$
		FR-8	F		<100	$1.8 \times 10^4$	$3.9 \times 10^5$
6	MI-6		M	ARG-Epuyen	>25,600	$6.5 \times 10^6$	$2.4 \times 10^7$
		MR-9	M		<100	$2.9 \times 10^4$	$5.5 \times 10^3$
7	FI-7		F	ARG-Epuyen	>25600	$4.1 \times 10^6$	$8.7 \times 10^2$
		FR-10	F		800	$1.2 \times 10^5$	$6.2 \times 10^6$
		FR-11	F		<100	ND	$3 \times 10^4$
8	MC-8		M	Mock-infected	0	0	0
		MR-12	M		0	0	0
9	FC-9		F	Mock-infected	0	0	0
		FR-13	F		0	0	0

\* hamsters found dead after a short symptomatic period

455

456

457

**Table 2.** Evaluation of amino acid changes of Andes virus strains.

Genomic segment, gene	Position	ANDV strain					
		CHI-9717869	CHI-7913	Andes/ARG, passage N°19	Epuyen/18 -19 (HPS case)	ARG-Epuyen, passage N°4	
<b>S-Segment</b>							
GenBank		MT956622	MT956618	OP555722	MN258238	PQ215668	
N	21	A	A	T	A	A	
NSs (ORF +1)	40	Q	Q	Q	R	R	
	47	N	N	N	S	S	
<b>M-Segment</b>							
GenBank		MT956623	MT956619	OP555727	MN258204	PQ215669	
Gn	97	S	S	P	S	S	
	114	I	I	V	I	I	
	216	F	F	F	L	L	
	353	T	V	V	I	I	
	499	V	V	V	I	I	
	641	T	T	T	I	I	
	Gc	938	T	A	T	A	A
		1055	S	S	A	S	S
		1115	V	V	V	I	I
		1127	V	V	I	V	V
<b>L-Segment</b>							
Gen Bank		MT956621	MT956620	OP555734	MN258171	PQ215670	
RdRp	141	T	I	I	V	V	
	144	R	R	K	R	R	
	364	N	N	N	S	S	
	402	I	V	V	I	I	
	541	A	A	V	A	A	
	876	S	S	S	A	A	
	1295	I	I	M	I	I	
	1440	S	S	S	N	N	
	1665	V	I	I	V	V	
	1675	P	P	S	P	P	
	1965	Q	Q	Q	H	H	
	2113	T	A	A	T	T	
	2116	K	K	K	K	E	

458

459

460 **FIGURES**

461 Figure 1. Visualization of ARG-Epuyen by Indirect immunofluorescence assay.

462 The micrograph shows Vero E6 cells infected with the ANDV ARG-Epuyen strain (p4,  
463 7 days post-infection), micrograph with DAPI, FITC and merge (A, B, C). Vero E6 cell  
464 control (mock infected cells), equal condition (D, E, F). Cells were stained with rabbit  
465 polyclonal serum against the nucleoprotein of ANDV, followed by an FITC-conjugated  
466 antibody against rabbit IgG. DAPI was used for DNA staining (4',6-diamidino-2-  
467 phenylindole). The images were captured at 400X magnification.

468

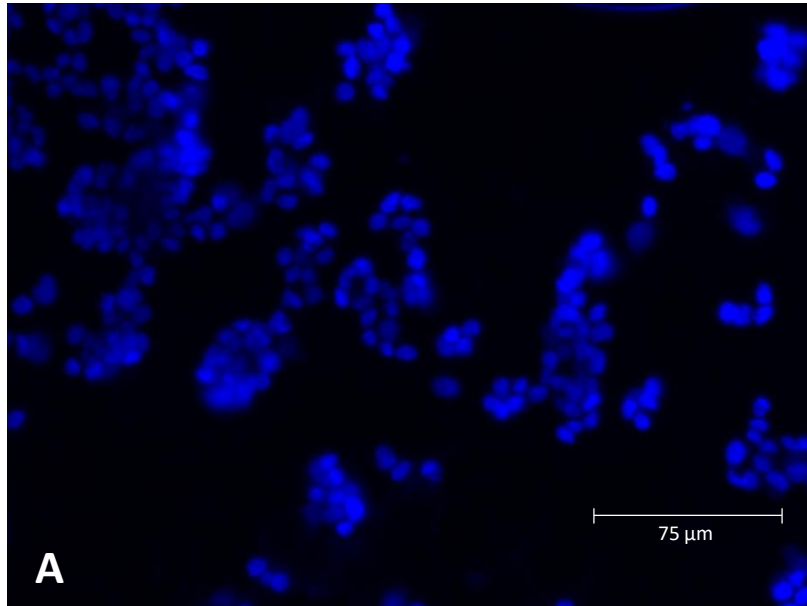
469 Figure 2. Comparative kinetics curves of Andes/ARG and ARG-Epuyen strains in Vero  
470 E6 (A) and comparative levels of infective viral particles of Andes/ARG and ARG-  
471 Epuyen strains in Vero E6 (B).

472

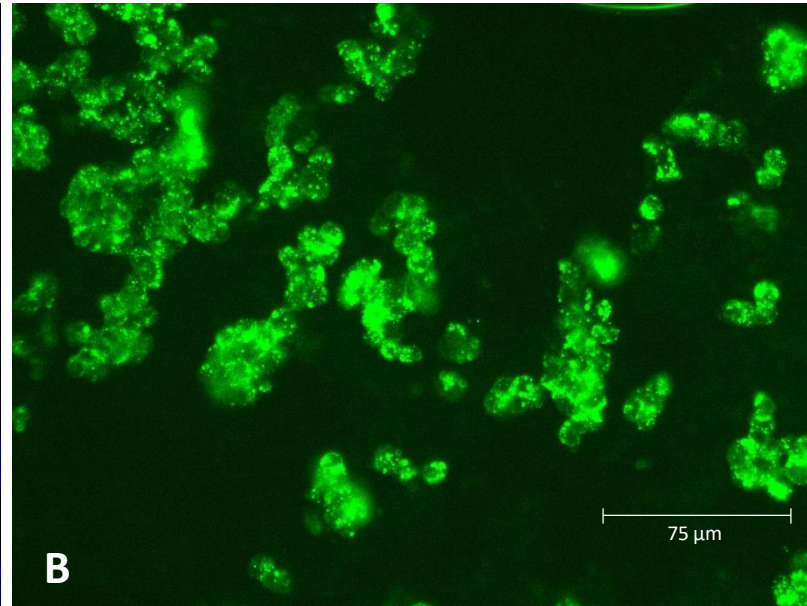
473 Figure 3. Comparative kinetics curves of ANDV strains in Vero E6 and A549 cells.

Figure 1

DAPI



FITC



MERGE

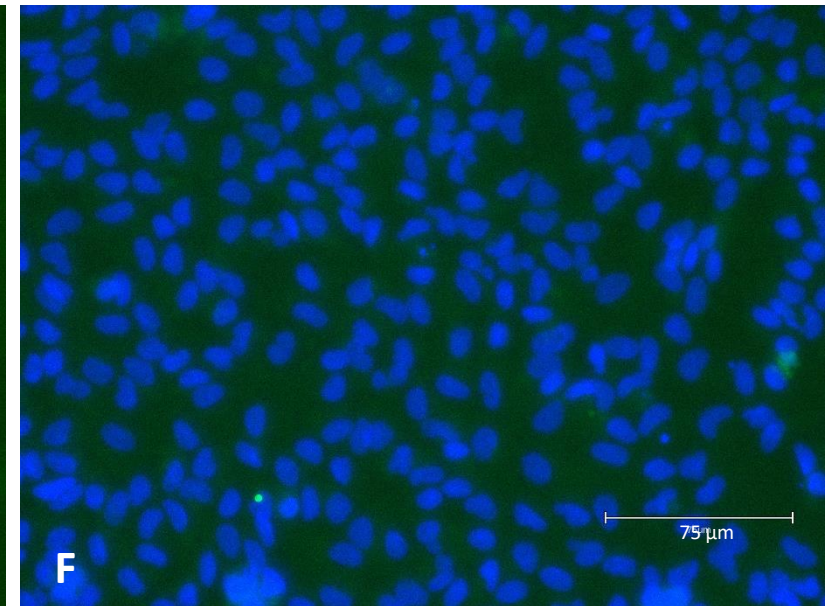
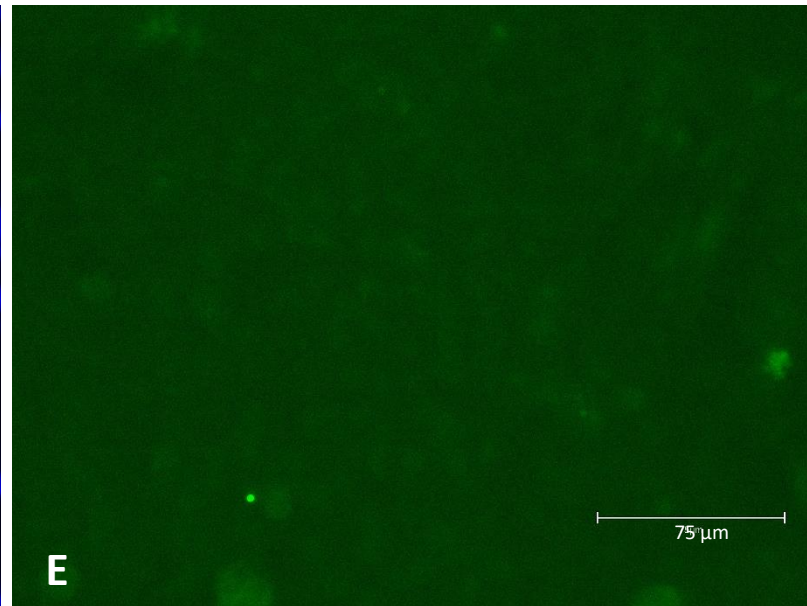
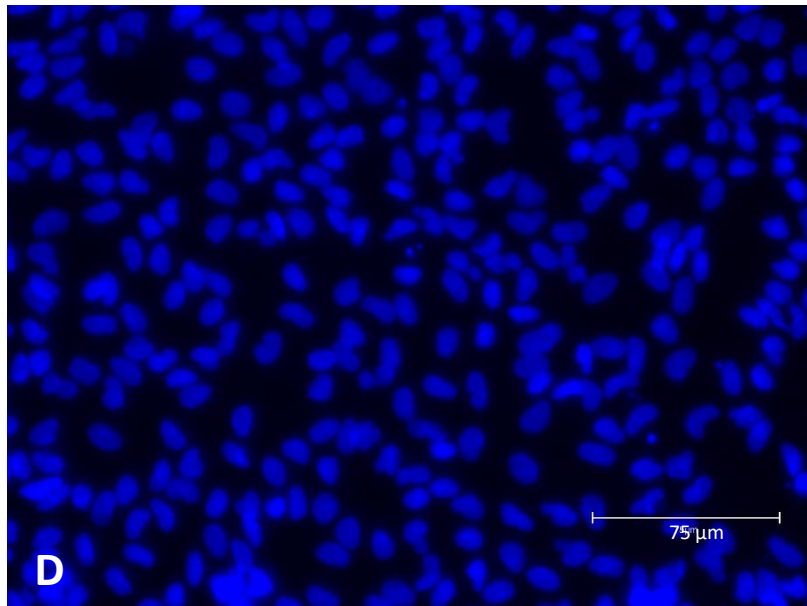
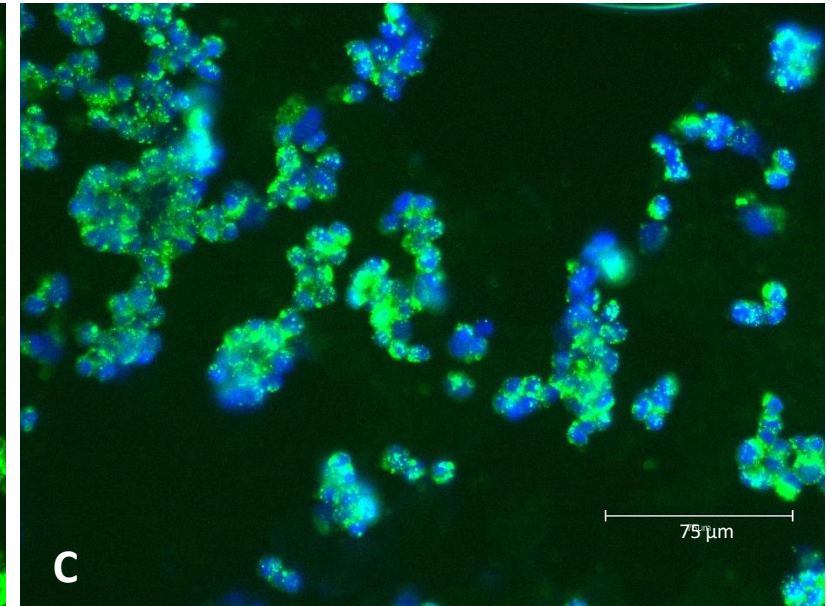
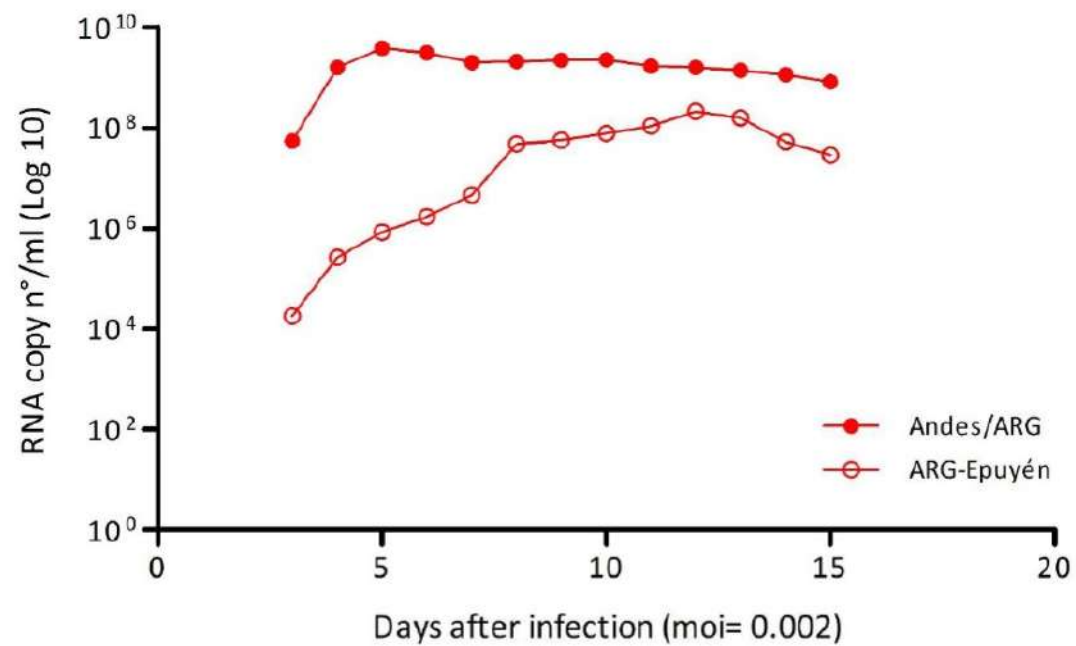
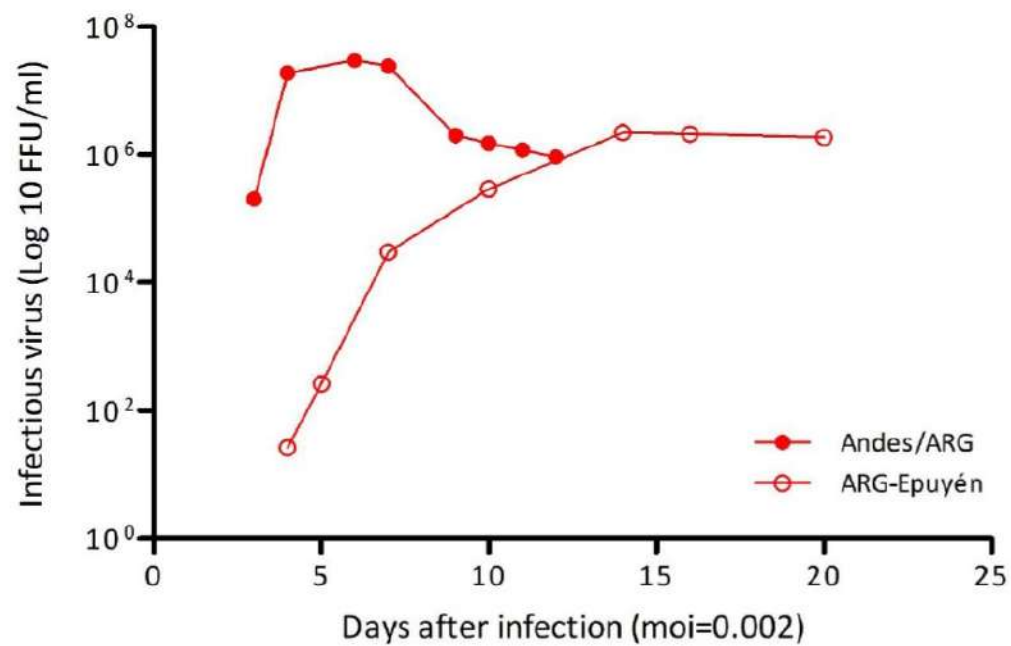


**Figure 2**



**A**



**B**

**Figure 3**

